Abstract：

A detailed experimental investigation of wall fires in underground confined space was conducted to study the heat fluxes under the ceiling. Various burner aspect ratios and fire heat release rates were employed to simulate different wall fire scenarios. The effect of source-ceiling height was also examined. The results show that the distribution of heat flux under the ceiling from fires on rectangular burners was significantly influenced by the burner aspect ratio. As the burner aspect ratio increased, the heat flux under the ceiling at a given position perpendicular to the side wall increased. It was found that the existing heat flux correlation developed for a square burner could not capture such influence as it did not include the burner aspect ratio. A new predictive model based on the equivalent burner diameter concept was proposed incorporating the burner aspect ratio and was shown to predict well the heat flux for all the cases with different heat release rates, burner aspect ratios and source-ceiling heights. The model was also validated against available data in the literature which were not used in its derivation. Further analysis was also conducted for the temperature contours constructed from the temperature measurements under the ceiling.

Keywords: Channel fire; wall fire; heat flux; aspect ratio; ceiling jet.

1. Introduction

Fires in reduced scale channels are often used to mimic fire scenarios in tunnels [1, 2], corridors [3] and underground spaces [4, 5]. The safety and security problems for such fires have raised widespread concern. Among them, the problem of ceiling fire prevention is of particular importance [6-9]. Typical confined channel fires often result in wall fires and ceiling jets, the characteristics of which are significantly different from unconfined fires.

Significant research has been carried out on the heat transfer mechanisms in ceiling jets [10-19]. Some pioneering work was performed by Alpert [10, 11], who conducted large-scale fire tests using an unconfined ceiling to investigate the ceiling jet characteristics of turbulent flames. You and Faeth [12, 13] also carried out experimental investigations of fire resulted ceiling jets in an unconfined environment. Using a square burner, they derived a correlation between the turbulent heat flux and the distance under the ceiling. Kokkala [14] tested natural gas fires under unconfined ceilings to measure ceiling heat flux. Chatterjee et al. [16] numerically simulated the ceiling flow under unconfined and inclined ceilings with FireFOAM, the large eddy simulation based fire solver within the frame of open source computational fluid dynamics code OpenFOAM. Johansson et al. [17] investigated the ceiling jet temperature and velocity profiles and proposed some correlations based on numerical experiments with the Fire Dynamics Simulator (FDS). Lattimer et al. [18, 19] conducted experiments on wall and corner flames to investigate the characteristics of flame heat flux when the walls were confined. More recently, Fan et al. [20] studied the temperature and heat flux characteristics of asymmetric hot plume channels with the restriction of sidewalls in small-scale tests.

Previous studies mostly focused on the ceiling heat flux induced by free fire plume under unconstrained or tunnel-like ceilings. Relatively little research has been performed on ceiling heat flux

distribution induced by wall fires in a channel. Furthermore, square or round fire sources were used in most previous research. This excluded the effects of the burner aspect ratio. There are many types of fire sources in practice. The shape of the fire source has some influence on the actual fire hazard. Similar rectangular wall fires are likely to occur in practice, e.g. a full burning car close to the wall in the channel shown below can be approximated as a rectangular fire close to the wall. The plume evolution and heat flux distributions induced by a rectangular fire source are expected to have some different characteristics from those on a square or round fire source. It is of relevance to the design of fire detection and suppression systems to quantify such characteristics.

2. Experiments

Figure 1 shows the experimental setup, which is a 1: 8 reduced scale model. The tests were carried out in a tunnel-lie channel constructed from fireproof panels with dimensions of 8 m (length) × 2 m (width) × 1 m (height). Four rectangular burners having the same surface area, but different aspect ratios were used to simulate the fire source from axisymmetric (n=1) to line (n=10) burners. The gas burners were made of stainless steel with dimensions of 12 cm × 12 cm, 20.8 cm × 6.9 cm, 29.4 cm × 4.9 cm and 38 cm × 3.8 cm, corresponding to aspect ratios of 1, 3, 6 and 10, respectively. The burner height was 15 cm. In the tests, the long side of the burner was aligned against the side wall to simulate wall fire under different conditions. The fuel was propane and the mass flow rate was controlled by a mass flow meter.
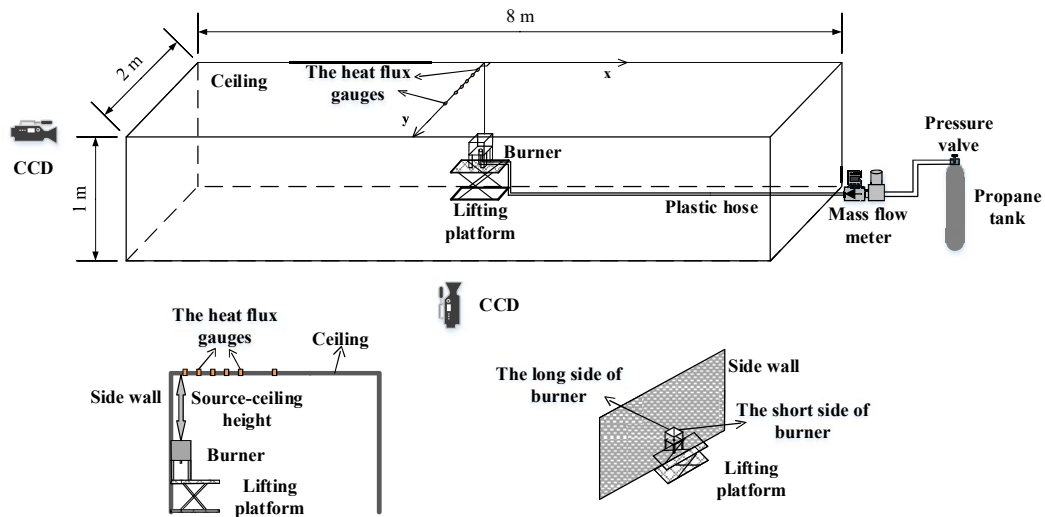
Fig. 1. The experimental setup.

The instrumentation is shown in Fig. 2. For heat flux measurements, six Gardon heat flux gauges were placed from above the ceiling by perforating it. The Gardon gauges were water-cooled and their measurement uncertainty was estimated to be ±3%. In order to measure the temperature distributions in the ceiling jet, 100 K-type thermocouples of 1 mm diameter were placed at 0.015 m below the ceiling.
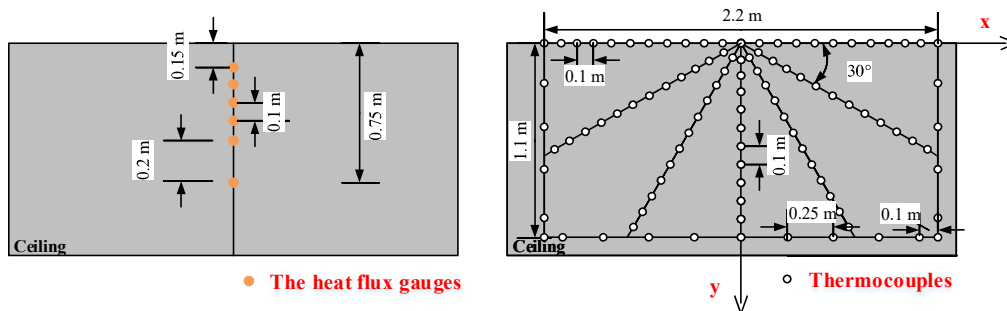

Fig. 2. The heat flux gauges and temperature measurement arrangements below the ceiling.

Table 1 summarizes the test conditions. All tests were performed in ambient temperatures of 25 ± 5 °C. The heat release rates (HRR), source-ceiling heights (H), and burner aspect ratios (n) were systematically varied to facilitate the investigations. The heat release rate was between 13.4 kW to

42.0 kW to ensure that the flames can reach the ceiling and spread along it in all conditions. Based on the Froude similarity criterion [21], the selected channel model size (1: 8) is equivalent to the full scale channel size of 64 m (length) × 16 m (width) × 8 m (height), which is in line with the size of the 4-lane channel in reality. The corresponding full-scale fire heat release rate is from 2.42 MW to 7.60 MW, which is also in line with the actual car fires. Considering all the experimental conditions, the Reynolds number ranged from 7.35×10^3 to 1.54×10^4 to ensure that the flames generated in the experiment were turbulent. In the experiment, heat flux data was collected in the stable section and the measurement time was 2 minutes. Each test with the same conditions was repeated three times. Very good repeatability was achieved with the differences between the original and repeated tests to be less than 10%. The average value of the measurements was taken as the measured value.

Table1 Experimental conditions

Test no.	Burner size L×W (cm ×cm)	Aspect ratio n (n= L/W)	Source-ceiling height H (m)	HRR (kW)	Re
1-18	12×12	1	0.28, 0.38, 0.48	13.4, 20.2, 25.2, 30.2, 35.3, 42.0	7.35×10^3 ~ 1.54×10^4
19-36	20.8×6.9	3	0.28, 0.38, 0.48	13.4, 20.2, 25.2, 30.2, 35.3, 42.0	7.35×10^3 ~ 1.54×10^4
37-54	29.4×4.9	6	0.28, 0.38, 0.48	13.4, 20.2, 25.2, 30.2, 35.3, 42.0	7.35×10^3 ~ 1.54×10^4
55-72	38×3.8	10	0.28, 0.38, 0.48	13.4, 20.2, 25.2, 30.2, 35.3, 42.0	7.35×10^3 ~ 1.54×10^4

3. Results and discussion

3.1 Heat flux distribution under the ceiling induced by wall fires with the square burner

Figure 3 shows the total heat flux distribution under the ceiling induced by wall fires with the

square burner under different source-ceiling heights and heat release rates. The total heat flux under the ceiling was found to increase with the increase of the heat release rate and decrease with the increase of the distance to the side wall. For different source-ceiling heights under the same heat release rate, the heat flux was found to decrease with the increase of the source-ceiling height.
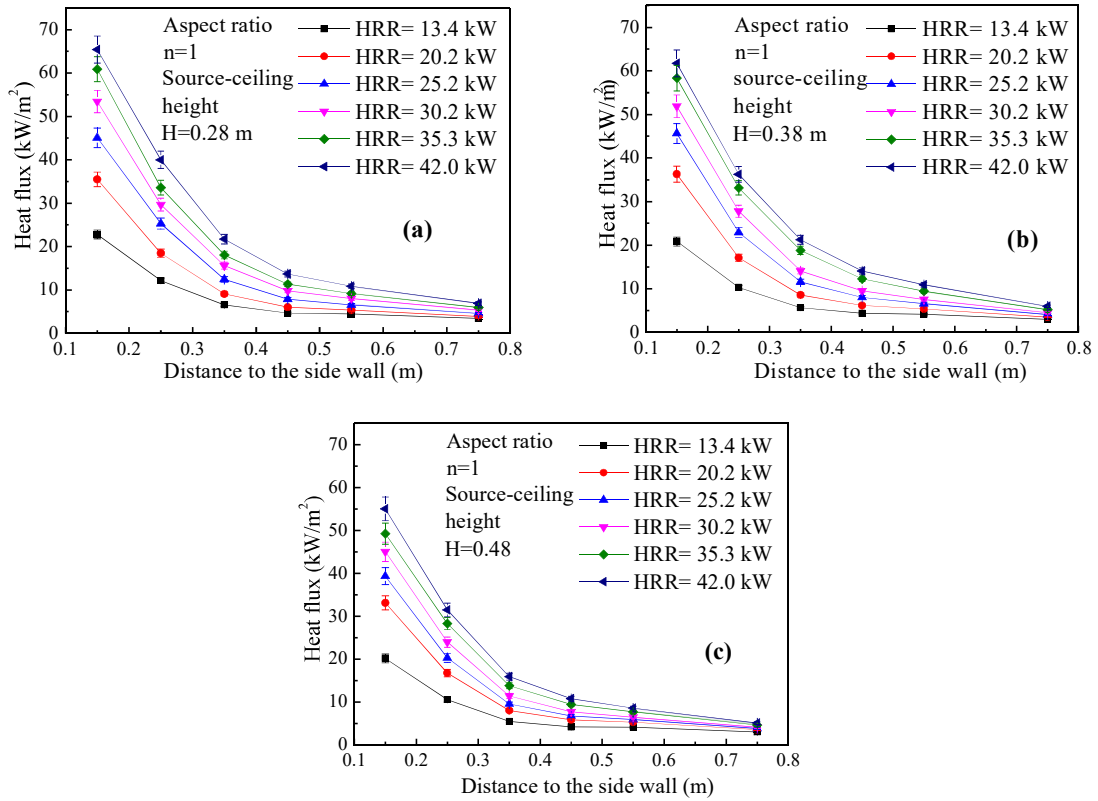

Fig. 3. The lateral heat flux distribution under the ceiling for wall fires induced by a square burner: (a) H=0.28 m; (b) H=0.38 m; (c) H=0.48 m.

It can be clearly seen from Fig. 3 that there are three factors influencing the heat flux distribution under the ceiling induced by a square burner wall fire, i.e. the distance to the side wall, the heat release rate and the source-ceiling height as noted in Eq. (1):

$$\dot{q}'' \propto f\left(H, \dot{Q}, r\right) \tag{1}$$

where $\dot{q}''$ is the total heat flux (kW/m^2), H is the source-ceiling height (m), $\dot{Q}$ is the total heat

release rate (kW), and r is the distance to the side wall (m).

Following [12, 13], heat flux and distance to the side wall can be cast into their dimensionless forms using the heat release rate and source-ceiling height as:

$$\frac{\dot{q}''H^2}{\dot{Q}} \propto f\left(\frac{r}{H}\right) \qquad (2)$$

The above equation was originally deduced for an open fire under the ceiling [12,13]. For a wall fire under the ceiling, Hasemi and Tokunaga [22] proposed the "mirror fire source" approach. They assumed that for restricted wall fires there was an "imaginary fire source" with the same intensity as the actual fire source on the other side of the wall. Comparing with the mass flow of the unconfined flame, the mass flow of the wall fire and the corner fire should be taken as 1/2 and 1/4 of the unconfined fire, respectively. With such assumption, they considered that the relationship represented by Eq. (2) could still hold for heat flux in the ceiling jet induced from a wall fire.

Figure 4 plots the dimensionless heat flux against the dimensionless distance to the side wall for all the cases with the square burner. Applying Eq. 2 for the data points and by fitting the data, the following equation can be obtained:

$$\frac{\dot{q}''H^2}{\dot{Q}} = 0.063\left(\frac{r}{H}\right)^{-1.525}, \frac{r}{H} > 0.2 \qquad (3)$$

The measurements of You and Faeth [12], which were not used in fitting the above correlations, were also included in Fig. 4 for comparison. The agreement between the measurements and predictions of the correlation is generally good. The measurements of You and Faeth [12] were generally smaller than the present measurements and the fitted correlation. This was thought to be due to the fact that there was no side-wall restriction in those tests[12], which only involved free fire impinging on the

ceiling. The presence of the side wall can influence the heat flux on the ceiling due to a combination of the resulting change in flame shapes as well as the changes in radiative and convective heat transfer.

The equation shown on the plot:

$$\frac{\dot{q}''H^2}{\dot{Q}} = 0.063\left(\frac{r}{H}\right)^{-1.525}$$
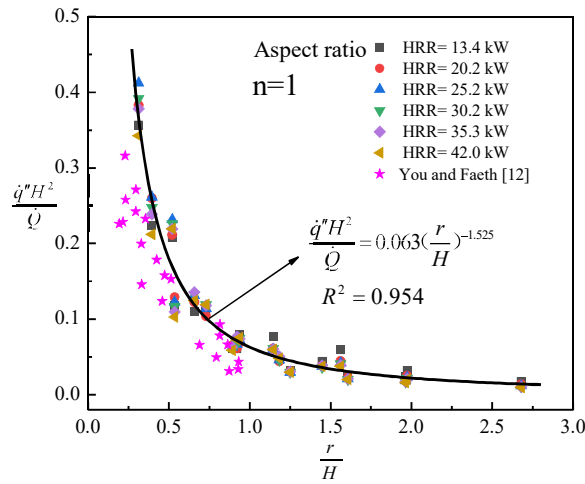
$$R^2 = 0.954$$

Fig. 4. Heat flux under the ceiling of wall fire induced by a square burner.
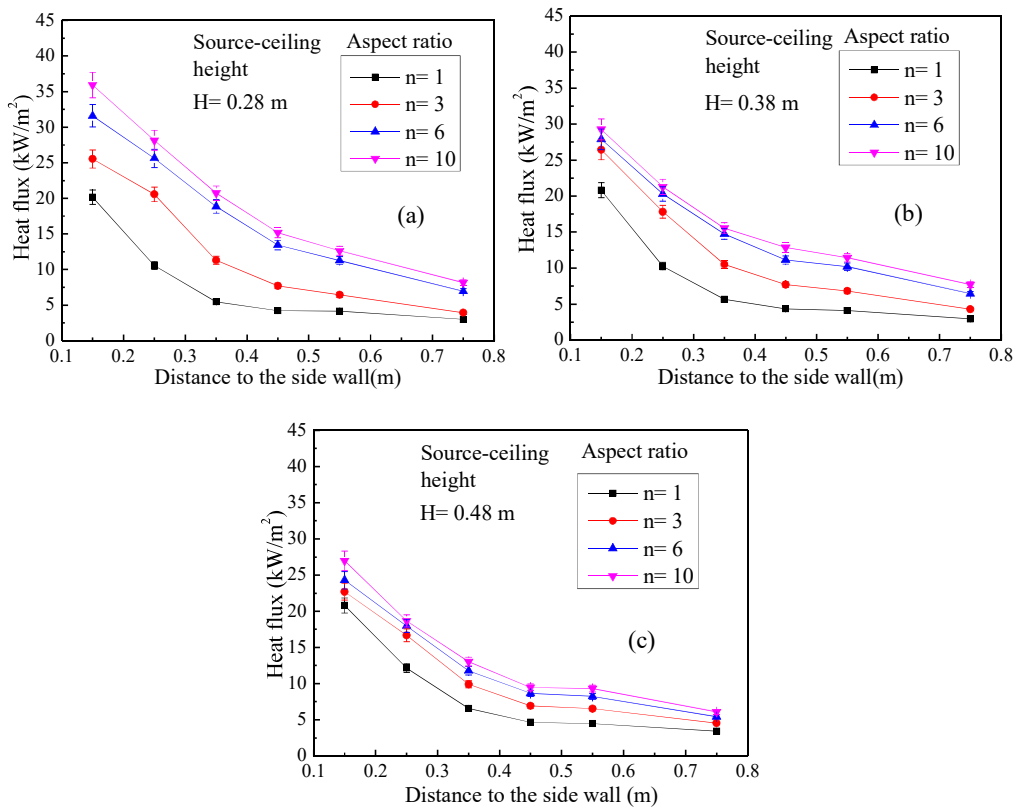

Fig. 5. Heat flux distribution under the ceiling induced by wall fires with different burner aspect ratios for a given heat release rates (HRR= 13.4 kW) but different source-ceiling heights.

3.2 Heat flux under the ceiling induced by wall fires with various burner aspect ratios

Figure 5 shows the total heat flux under the ceiling induced by wall fires with different burner aspect ratios at the same heat release rates but different source-ceiling heights. It was found that the lateral heat flux under the ceiling gradually increased as the burner aspect ratio increased. When the source-ceiling height increased, the change of the burner aspect ratio still affected the total heat flux but to a less extent.

Figure 6 shows the flame appearance probability contour of burners with different aspect ratios from the front and side view. An image processing program was constructed to obtain the flame appearance probability. Firstly, the transient flame evolutions were captured by the CCD camera with 1920 ×1080 pixels and 25 frames per second. For each test, 30 s of the original videos with a constant heat release rate were decompressed into 750 consecutive frames. Then the OTSU method [23], which is a threshold selection method from grey-level histogram, was programmed through MATLAB and used to convert the original frames into the grey scale images. The threshold obtained was used to identify the flame area in each image. By averaging all the captured frames, the visible flame appearance probability was obtained. Finally, the colour contours were obtained by changing the colour scheme.   For a strong plume impinging upon the ceiling, the variation of the flame extension length along the side view direction is not obvious for a given HRR and source-ceiling height. The fire plume can be divided into the vertical sections against the side wall and the horizontal diffusion stage on the ceiling. It can be further assumed that the flame surface area is the sum of the flame area against the sidewall and ceiling flame spread area. The flame area against the sidewall can be approximated as of rectangular shape as shown in Fig. 6b. It increased with the increase of the burner aspect ratio in the front view direction, which is an important factor causing the difference in heat flux under the

ceiling. However, thermal radiation from the main flame volume would have greater influence on the heat flux on the ceiling along the side view than the front view direction. Hence, the lateral heat flux under the ceiling gradually increased with the increase of the burner aspect ratio.
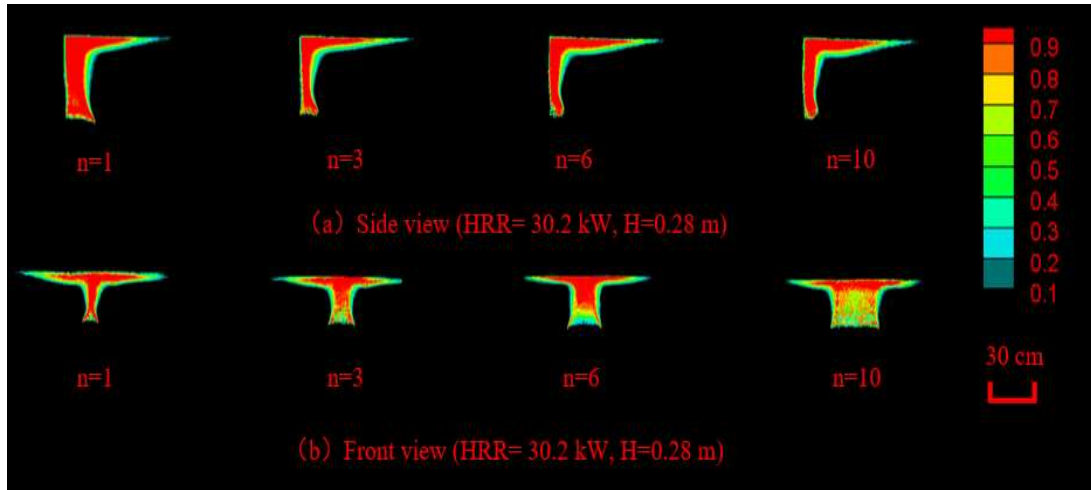

Fig. 6. Flame appearance probability contour for burners with different aspect ratios from the front and side view.

Following the same procedure for the square burner case, Equation 2 was applied to these measurements involving different aspect ratios. As shown in Fig. 7, the data points can no longer collapse to one curve. The relationships between the dimensionless heat flux and distance to the wall change with the burner aspect ratio. In addition, the fitted curves for different burners also showed some irregularity. As the burner aspect ratio increases, the fitted curve becomes more gentle. In order to consider the effect of burner aspect ratio, it was hence decided to introduce a dimensionless size factor.
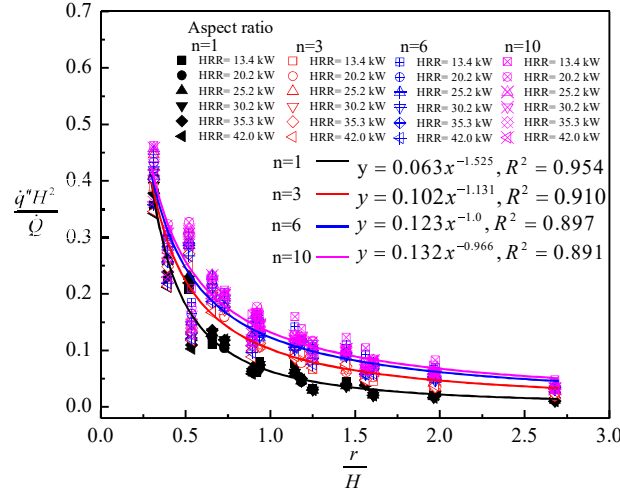
Fig. 7. The relationship between dimensionless heat flux and dimensionless distance for burners with various aspect ratios.

The hydraulic diameter D is often used to characterize rectangular sources. The relationship between the hydraulic diameter D, the area of the fire source S and the aspect ratio ($n=L/W$) is as follows:

$$D = \frac{4S}{p} = \frac{4S}{2(L+W)} = \frac{2S^{1/2}}{(n^{1/2} + n^{-1/2})} \qquad (4)$$

Consequently, the total heat flux under ceiling induced by wall fire plume can be expressed as:

$$\dot{q}'' \propto f\left(H, \dot{Q}, r, D\right) \qquad (5)$$

Following You and Faeth [12], the left-hand side of Eq. (5) can be simplified to $\dfrac{\dot{q}''H^2}{\dot{Q}}$, then the right side of the Eq. (5) would be dimensionless. Thus, Eq. (5) can be further simplified as:

$$\frac{\dot{q}''H^2}{\dot{Q}} \propto f\left(\frac{r}{H}, \frac{D}{H}\right) \qquad (6a)$$

$$\text{or,} \quad \frac{\dot{q}''H^2}{\dot{Q}} \propto f\left(r/H, \left(\frac{2S^{1/2}}{(n^{1/2} + n^{-1/2})}\right)\Big/H\right) \qquad (6b)$$

12

Examining Fig. 7 in detail, it can be seen that the second parameter on the right-hand side of Eq.6, i.e. the aspect ratio of rectangular burner, plays a key role in the relationship. In order to account for the effect of burner aspect ratio (or equivalently of the aspect ratio), an empirical factor $\exp\left[\frac{10}{3}\left(\frac{D}{H}\right)\right]$ was introduced following Lee et al. [24], who studied flame height and heat flux on facades and proposed a correlation of heat fluxes on facades by including an empirical correction $\exp\left[0.6\left(H_3/\ell_1\right)\right]$ to account for a residue effect of the aspect ratio, where H_3 is the opening height and ℓ_1 is characteristic radius of opening involving the aspect ratio of opening. Finally, all the current measurements for rectangular burners with different aspect ratios were plotted in Fig. 8. The data points collapsed to one curve. For comparison, measurements from previous work of Lattimer et al. [19] studying heat fluxes under ceiling with various heat release rates and source-ceiling heights (H) were also plotted in Fig. 8. The comparison confirms that the correlation determined in this work is valid when the abscissa (r/H) is greater than 0.2. Although further validation against more measurements would also be desirable.

$$\frac{\dot{q}''H^2}{\dot{Q}}\exp\left[\frac{10}{3}\left(\frac{D}{H}\right)\right]=0.4\left(\frac{r}{H}\right)^{-1}, \qquad \frac{r}{H}>0.2 \tag{7}$$
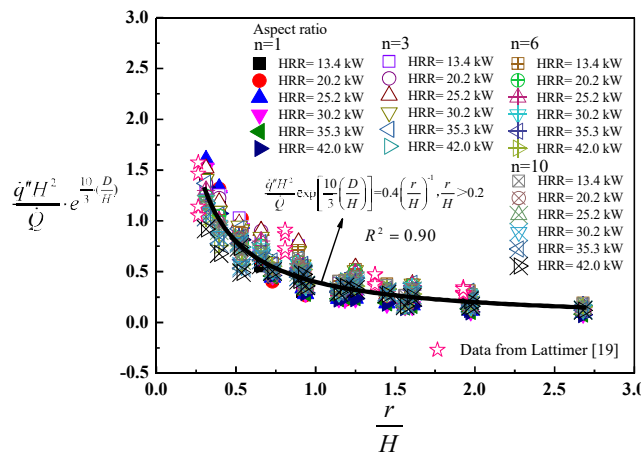

Fig. 8. A new correlation of dimensionless heat flux under ceiling accounting for burner aspect ratios in a channel.

3.3 Temperature distribution under the ceiling of wall fire induced by burners of different aspect ratios

Figure 9 shows the temperature contours from measurements at 0.015 m below the ceiling for the burners with different aspect ratios. For the temperature measurements, each test was repeated 3 times. The measurement time for temperature was 2 minutes; the measurements were conducted in the stable section. It can be clearly seen that as the burner aspect ratio increases, the temperature in the y-axis direction of the ceiling (i.e. perpendicular to the direction of the side wall) also increases. This trend is consistent with the finding in the ceiling heat flux.

Since the heat flux is linked with the temperature, the relationship between the ceiling heat flux and the burner aspect ratio can also be inferred from the obtained temperature contour map. In the direction perpendicular to the side wall, the heat flux and temperature under the ceiling increase as the aspect ratio of the burner increases. In the direction along the side wall, the temperature under the ceiling tends to decrease as the aspect ratio of the burner increases.
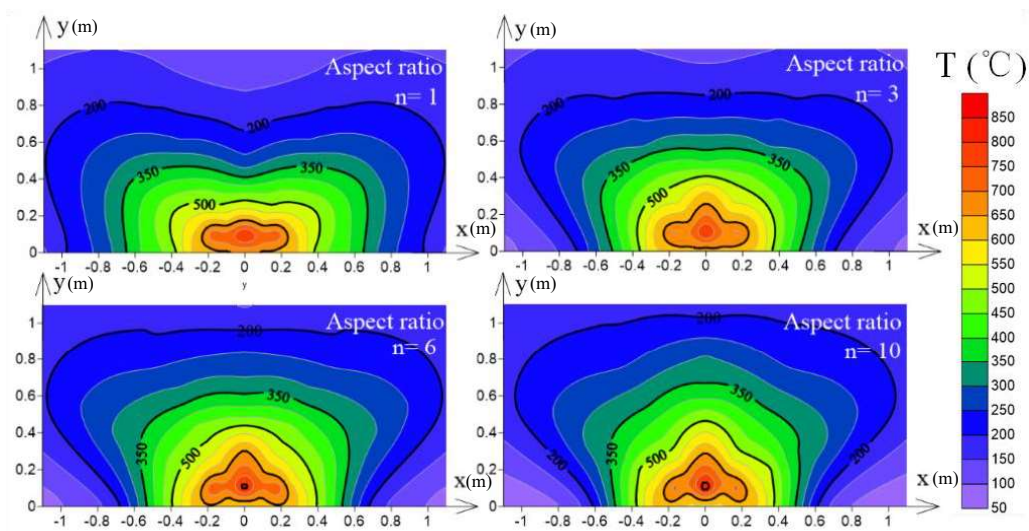

Fig. 9. Temperature contour map with different burner aspect ratio under the ceiling

(H= 0.38 m, HRR= 30.2 kW).

4. Conclusions

The heat flux distribution induced by wall fires with various burner aspect ratios in a channel were experimentally investigated with a specially designed test rig. A series of tests were conducted by systematically changing the fire heat release rate, source-ceiling height and the burner aspect ratio. Measurements were taken for the heat flux and the temperature under the ceiling. It was found that the impinging ceiling jet resulted from the wall fire induced by a rectangular burner with larger aspect ratios were significantly different from previously wall fires on square burners. The main findings can be summarized as follows:

(1) For the square burner, the heat flux under the ceiling increased as the heat release rate of the fire source increased, whereas it decreased as the distance to the side wall increased. The source-ceiling height also affected the heat flux under the ceiling. As the source-ceiling height increased, the heat flux decreased.

(2) For burners with different aspect ratios, the heat flux under the ceiling gradually increased as the burner aspect ratio increased, indicating that the aspect ratio of the fire source had some influence on the heat flux distribution under the ceiling.

(3) Considering the differences in the measurements for different burner aspect ratios, a new correlation was proposed for the heat fluxes under the ceiling induced by wall fires with different burner aspect ratios in a channel. The temperature contours under the ceiling were also analysed and compared with the heat flux distribution field map to verify the findings.

References

[1] F. Tanaka, K. Fukaya, K. A. M. Moinuddin, Development of a technique for establishing a pseudo tunnel length, Proc. Combust. Inst. 37(2019) 3985-3992.

[2] H.Y. Cong, X.S. Wang, X.X. Kong, H.L. Xu, Effects of fire source position on smoke extraction efficiency by natural ventilation through a board-coupled shaft during tunnel fires, Proc. Combust. Inst. 37(2019)3975-3984.

[3] W.G. Bos, T.V.D. Elsen, C.J. Hoogendoorn, F.L. Test, Numerical study of stratification of a smoke layer in a corridor, Combust. Sci. Technol. 38 (1984) 227-243.

[4] P. Ntzeremes, K. Kirytopoulos, Applying a stochastic-based approach for developing a quantitative risk assessment method on the fire safety of underground road tunnels, Tunnel. Undergr. Space Technol. 81(2018) 619-631

[5] Y.Z. Li, H. Ingason, Overview of research on fire safety in underground road and railway tunnels, Tunnel. Undergr. Space Technol. 81(2018)568-589.

[6] X.C. Zhang, L.H. Hu, W. Zhu, X.L. Zhang, L.Z. Yang, Flame extension length and temperature profile in thermal impinging flow of buoyant round jet upon a horizontal plate, Appl. Therm. Eng., 73 (2014) 15-22.

[7] Y. Huo, Y. Gao, W.K. Chow, A study on ceiling jet characteristics in an inclined tunnel, Tunn. Undergr. Space Technol., 25 (2010) 122-128.

[8] Z.H. Gao, J. Ji, H.X. Wan, K.Y. Li, J.H. Sun, An investigation of the detailed flame shape and flame length under the ceiling of a channel, Proc. Combust. Inst., 35 (3) (2015) 2657-2664

[9] H.W. Ding, J.G. Quintiere, An integral model for turbulent flame radial lengths under a ceiling, Fire Saf. J. 52 (2012) 25-33.

[10] R.L. Alpert, Turbulent ceiling-jet induced by large-scale fires, Combust. Sci. Technol. 11 (1975) 197–213.

[11] R.L. Alpert, Convective Heat Transfer in the Impingement Region of a Buoyant Plume, J. Heat Transfer. 109(1987) 120–124.

[12] H.Z. You, G.M. Faeth, Ceiling heat transfer during fire plume and fire impingement, Fire Mater. 3 (3) (1979) 140–147.

[13] H.Z. You, An investigation of fire-plume impingement on a horizontal ceiling 2— Impingement and ceiling-jet regions, Fire Mater. 9 (1) (1985) 46–56.

[14] M. Kokkala, Experimental study of heat transfer to ceiling from an impinging diffusion flame, Fire Saf. Sci. 3 (1991) 261–270.

[15] Y. Oka, O. Imazeki, O. Sugawa. Temperature profile of ceiling jet flow along an inclined unconfined ceiling, Fire Saf. J. 45 (2010) 221-227.

[16] P. Chatterjee, K.V. Meredith, Y.   Wang, Temperature and velocity distributions from numerical simulations of ceiling jets under unconfined, inclined ceilings, Fire Saf. J. 91 (2017) 461-470.

[17] N.   Johansson, J. Wahlqvist, P.V. Hees. Numerical experiments in fire science: a study of ceiling jets, Fire Mater. 39 (2015) 533-544.

[18] B.Y. Lattimer, U. Sorathia, Thermal characteristics of fires in a noncombustible corner, Fire Saf. J. 38 (2003) 709–745.

[19] B. Y. Lattimer, C. Mealy, J. Beitel, Heat fluxes and flame lengths from fires under ceilings, Fire Technol. 49 (2) (2013) 269-291.

[20] C.G. Fan, J.Q. Zhang, K.J. Zhu, K.Y. Li, An experimental study of temperature and heat flux in a channel with an asymmetric thermal plume, Appl. Therm. Eng. 113 (25) (2017) 1128-1136.

[21] J.G. Quintiere, Scaling Applications in Fire Research. F. Saf. J. 15(1989)3-29

[22] Y. Hasemi, T. Tokunaga, Some experimental aspects of turbulent diffusion flames and buoyant plumes from fire sources against a wall and in a corner of walls, Combust. Sci. Technol. 40 (1984) 1-4.

[23] N. Otsu, A threshold selection method from gray-level histogram. IEEE Trans Syst Man Cybern. 1979.

[24] Y.P. Lee, M. Delichatsios, G. Silcock, Heat fluxes and flame heights in facades from fires in enclosures of varying geometry, Proc. Combust. Inst. 31 (2007)2521–2528.